LAWRENCE LIVERMORE NATIONAL LABORATORY

LLNL-JRNL-655829

Karhunen-Loeve expansion analysis of uncertainties in could microphysical property retrievals

X. Chen, Q. Tang, S. Xie, C. Zhao

June 16, 2014

Geophysical research letters

LLNL-JRNL-655829

Karhunen-Loéve expansion analysis of uncertainties in cloud microphysical property retrievals

X. Chen,[1] Q. Tang,[2] S. Xie[2] and C. Zhao[3]

X. Chen, Center for Applied Scientific Computing, Lawrence Livermore National Laboratory, 7000 East Ave., Livermore, California 94550, USA. (chen73@llnl.gov)

Q. Tang, AEED-Atmospheric, Earth and Energy, Lawrence Livermore National Laboratory, 7000 East Ave., Livermore, California 94550, USA. (tang30@llnl.gov)

S. Xie, AEED-Atmospheric, Earth and Energy, Lawrence Livermore National Laboratory, 7000 East Ave., Livermore, California 94550, USA. (xie2@llnl.gov)

C. Zhao, College of Global Change and Earth System Science, Beijing Normal University, XinJieKouWai Street, No. 19, Beijing, 100875, China. (czhao@bnu.edu.cn)

[1]Center for Applied Scientific Computing,
Lawrence Livermore National Laboratory,
Livermore, California, USA.

[2]AEED-Atmospheric, Earth and Energy,
Lawrence Livermore National Laboratory,
Livermore, California, USA.

[3]College of Global Change and Earth
System Science, Beijing Normal University,
Beijing, China.

This study proposes a methodology of quantifying uncertainties for cloud retrievals on model resolution to facilitate the comparison with model outputs. Primary component analysis is applied to reduce the dimension of random variables (up to a factor of 50) and reveal the cross correlations in the input data, making large sampling computationally feasible and uncertainty quantification accurate and reliable. Our approach has the capability of parameterizing input uncertainties and attributing the uncertainties in the retrieval output to each individual source, which allows sensitivity analysis of cloud retrieval algorithms and provides directions for improving observation instruments as well as strategies. We applied the method to characterize uncertainties in cloud ice water content (IWC) retrieved from the DOE Atmospheric Radiation Measurement (ARM) programs baseline cloud microphysical retrieval algorithm (MICROBASE). We test it with a selected ice cloud case observed on 9 March 2000 at the ARM Southern Great Plains site during its 2000 cloud intensive observing period. The test results indicate that (1) uncertainties in the output retrieved by MICROBASE are comparable amongst different retrievals; (2) The mean values obtained by our UQ method are closer to the aircraft data with less errors compared to the direct ensemble average; (3) Ice water path (IWP) generally incurred larger uncertainty in optically thin ice clouds and there was more variability in vertical in the retrieved IWC; and (4) Uncertainties in the output are mainly due to the interactions among different modes of ARM radar profiles.

1. Introduction

Cloud properties such as liquid and ice water contents retrieved from ground-based measurements have been widely used in climate model evaluation, however, earlier studies have shown that there exist large differences and uncertainties in ground-based cloud retrievals, (e.g., [*Comstock et al.*, 2007; *Turner et al.*, 2007; *Zhao et al.*, 2012]). They indicated that these differences and uncertainties are primarily from the retrieval theoretical bases, assumptions, as well as input profiles and constraint parameters. Quantifying the uncertainty in cloud retrievals has been long desired from the developer and user communities [*Xie*, 2011]. One way to quantify the uncertainty in a particular cloud retrieval product is through calculating the variability based on ensemble average of retrieved cloud properties [*Comstock et al.*, 2007]. Another way is through perturbing input profiles and several key parameters used in the retrieval algorithm, as demonstrated in [*Zhao et al.*, 2014], which applied a simple perturbation method to the ARM program baseline retrieval of cloud microphysical properties (MICROBASE [*Dunn et al.*, 2011]).

However, the classical uncertainty analysis methods for quantifying the uncertainty in cloud retrieval often suffers from the following limitations: (1) correlations among various influential factors may not be considered; (2) parametrizing input profiles with corresponding correlations may not be an obvious task; (3) sampling random variables amongst various vertical layers may require large number of samples; (4) characterizing *a-priori* probability density function still requires some unnecessary statistical assumptions; and (5) attributing contribution of variability in the retrieved product to each individual source is not permitted in general. To address these issues, this study aims to establish a novel observation-based methodology to generally quantify the retrieval uncertainties for model evaluation (especially global models) over a typical model temporal resolution, i.e., 30 minutes. This method is based on Karhunen-Loéve (KL) expansion (KLE) [*Kuhunen*, 1947; *Loéve*, 1945] and Central Limit Theorems (CLT) [*Ross*, 2010] to quantify the uncertainties introduced by potential errors in measurements and uncertainties in parameters used in cloud retrievals. Our approach takes account for the correlation between vertical layers in the input profiles and reduces the number of random variables, which renders large sampling computationally feasible and makes output uncertainty range results accurate and reliable. This approach is to make objective comparison between observations and model outputs according the formulations of climate models and definition of retrieval algorithm defined as a space-time average for a specific spatial-temporal domain, such as 1 degree $\times$ 1 degree $\times$ 30mins. Despite that many existing methods can only estimate column-integrated uncertainties, our unique method also provides vertically resolved UQ analysis, which are essential to many topics, such as radiative forcing and climate change. We also implement the sensitivity analysis of retrieved quantity of interest with respect to each individual source, which are particularly useful when dealing with highly non-linear retrieval algorithms, as different error sources are more likely entangled.

The structure of the paper is as follows. In Section 2, the details of KLE-CLT based uncertainties analysis in cloud microphysical property retrievals are given. In Section 3, the method is tested with a ice cloud case observed on 9 March 2000 at the ARM SGP Climate Research Facility to quantify uncertainties of cloud ice water content (IWC) using MICROBASE as the retrieval algorithm. Results from our uncertainty analysis and sensitivity studies are shown in Section 4. Finally, we provide directions in Section 5 for improving observation instruments as well as strategies.

2. Methodology

KLE is usually used to solve stochastic problem involving large number of random variables with stable correlation kernel during an observation period, while CLT is generally used to deal with unknown *a-priori* probability density functions of random variables. We will combine KLE and CLT to propagate the uncertainties from ground-based measurements as well as the empirical parameters through MICROBASE retrieval algorithm. MICROBASE is the ARM baseline retrieval for cloud properties based on the cloud radar and lidar measurements [*Dunn et al.*, 2011; *Zhao et al.*, 2014]. It derives the liquid and ice properties using empirical regression equations obtained from in situ aircraft measurements with some assumptions. Liquid water content (LWC) and ice water content (IWC) are derived from radar reflectivity at 35 GHz and some empirical parameters, where LWC is retrieved by $LWC = LWP\frac{Ze_{Liq}^{g}}{\sum_{i=1}^{n} Ze_{Liq}^{g}\Delta Z}$, while for pure ice clouds, IWC is retrieved by $IWC = aZe_{Ice}^{b}$. In the equations above, a, b and g are empirical parameters, and ΔZ is the increment in vertical. Uncertainties in its retrieved cloud property comes from three sources: input profiles, retrieval algorithm, and assumptions as described in [*Zhao et al.*, 2012, 2014].

To start with, we introduce a temporal-spatial stochastic process $Y(\mathbf{x}, t, \theta)$ to represent unbiased raw observations (e.g., radar reflectivity profiles to be described in Section 3, where $\mathbf{x}$ denotes the height, t denotes the time, and θ represents a random event). As a result, an ensemble of snapshots of the stochastic process $Y(\mathbf{x}, t, \theta)$ observed in the analysis time window $[0, T]$ can be recorded as $\{y_1, y_2, \ldots, y_n\}$, where $y_i(\mathbf{x}) = y(\mathbf{x}, t_i)$, $i = 1, \ldots, n$, n is the number of snapshots; and the ensemble average of the snapshots can be defined as $\bar{y}(\mathbf{x}) = \frac{1}{n}\sum_{i=1}^{n} y_i$.

With noises added to unbiased raw stochastic process $Y(\mathbf{x}, t, \theta)$, we have input profiles $Y'(\mathbf{x}, t, \theta)$, defined as $Y'(\mathbf{x}, t, \theta) = Y(\mathbf{x}, t, \theta) + \text{noise}$. Since $Y(\mathbf{x}, t, \theta)$ can be decomposed into ensemble average $\bar{y}(\mathbf{x})$ and an unknown random estimation error $\epsilon(\mathbf{x}, t, \theta)$, such that $Y(\mathbf{x}, t, \theta) = \bar{y}(\mathbf{x}) + \epsilon(\mathbf{x}, t, \theta)$. Therefore, we obtain

$$Y'(\mathbf{x}, t, \theta)) = \bar{y}(\mathbf{x}) + \epsilon(\mathbf{x}, t, \theta) + \text{noise} \tag{1}$$

The goal of this paper to make objective comparison between observations and model outputs according the formulations of climate models and definition of retrieval algorithm defined as a space-time average for a specific spatial-temporal domain such as 1 degree $\times$ 1 degree $\times$ 30mins. Thus, input profiles $Y(\mathbf{x}, t, \theta)$ and $Y'(\mathbf{x}, t, \theta)$ are transformed to more smooth statistic $\overline{Y}(\mathbf{x}, t, \theta)$ and $\overline{Y'}(\mathbf{x}, t, \theta)$ (sample mean of $Y(\mathbf{x}, t, \theta)$ and $Y'(\mathbf{x}, t, \theta)$ within the time window), respectively, whose probability density functions are approximately normal (to be discussed in the subsequent paragraphs).

Due to the high dimensionality of the stochastic space for $Y(\mathbf{x}, t, \theta)$ (e.g., 512 vertical layers in ARM radar reflectivity profiles), it is computationally infeasible to sample all the vertical layers. To reduce the dimensionality, we applied KLE to represent the stochastic process $Y(\mathbf{x}, t, \theta)$ in terms of eigenfunctions of its correlation kernel assuming it is piece-wise stable within the analysis time window. The detailed derivations can be found in Appendix A. The method was originated in [*Pearson*, 1901]. *Hotelling* [1933]; *Kosambi* [1943] introduced the principal component analysis (PCA) which involves a statistical procedure that transforms a number of possibly correlated variables into a smaller number of uncorrelated variables called principal components. In practice, the correlation kernel is approximated numerically by constructing a covariance matrix using the method of snapshots [*Sirovich et al.*, 1987] within a time window.

Based on Central Limit Theorems [*Ross*, 2010], random variables appeared in the KL expansion of $\overline{Y}(\mathbf{x}, t, \theta)$ approximately follow student or normal distribution when sample size is large enough (large number law). By truncating KL expansion of $\overline{Y}(\mathbf{x}, t, \theta)$ to the order of M and adding white noises, we obtain the corresponding $\overline{Y'}(\mathbf{x}, t, \theta)$ that can be written as

$$\overline{Y'}(\mathbf{x}, t, \theta) = \bar{y} + \sum_{i=1}^{M} \psi_i \sqrt{\frac{\lambda_i}{n}} \sqrt{1 + \left(\frac{\sigma_0}{\sqrt{\frac{\lambda_i}{n}}} \right)^2} \frac{z_i}{\sqrt{n}} \tag{2}$$

where $z = [z_1, z_2, \ldots, z_M]^{\mathbf{T}}$, $z \sim \mathcal{N}(0, \mathbf{I}_M)$ and $\mathbf{I}_M$ is a $M \times M$ identity matrix. The detailed proof is given in the Appendix B. To simplify, other than observation-based input profiles, uniform distributions are applied for perturbing algorithm and assumption parameters of the retrieval. We will apply Sobol' [*Sobol*, 1993] method to derive global sensitivity analysis of microphysical properties retrieved by MICROBASE. Sobol' method is a variance-based sensitivity analysis method, which divides the variance of the output into fractions attributed to each input (first-order indices) and their interactions (second- or higher-order indices). The fractions measure the contribution to the output variances of each input variable, including all interactional variances with any other input variables in all the orders. Also, Latin Hypercube Sampling (LHS) procedure is used to draw samples in the designed space for input profiles and parameters. LHS is an effective stratified sampling approach in a high-dimensional space ensuring that all portions of a given partition are sampled [*McKay et al.*, 1979].

3. Application

To demonstrate the value of the proposed uncertainty analysis method, we apply it to quantify uncertainty in MICROBASE retrieved ice properties for high cirrus cloud case observed on 9 March 2000 at the ARM SGP site during the 2000 cloud intensive observing period (IOP). The cirrus cloud case has been studied comprehensively in [*Comstock et al.*, 2007] to examine the ability of 15 state-of-art cloud retrievals to retrieve ice cloud properties. As described in [*Comstock et al.*, 2007] , the cirrus cloud observed on 9 March 2000 formed as a weak upper-level disturbance and propagated over the SGP region in a strong southwesterly flow. The initial cloud formation occurred as the weak disturbance passed over the mountains of central New Mexico during the local morning of 9 March. The clouds thickened into a series of bands oriented along the wind as the disturbance moved northeastward. The visible optical depth varied by two orders of magnitude over the 3.5-hour time period, which is typical for midlatitude synoptically generated frontal cirrus clouds that tend to be initially optically thin and increase in optical thickness as the cloud system passes overhead. The majority of the cloud observed during the 9 March 2000 case falls into this optically thick category. Optically thin ice clouds only occurred during the (1900–1915UTC, 22:00–2230 UTC) period displayed in Figure 1 (a).

Comstock et al. [2007] has shown large uncertainties in the retrieved ice cloud properties among the tested algorithms for both optically thin ($\tau < 0.3$) and thick ($0.3 < \tau < 5.0$) cirrus clouds. The measurement error σ_0 of radar reflectivity profiles in equation (2) is about 0.5 dBZ, which is the instrument error. The empirical parameter a is assumed to follow uniform distribution in the range of 0.03 to 0.22 with the unit $(\mathrm{g/m^3})$ /dBZ, while the empirical parameter b is assumed to be a dimensionless number defined as 0.59.

The spatial-temporal image of radar reflectivity profiles observed on 9 March 2000 at the ARM SGP is plotted in the Figure 1 (a). Using KL expansion, we reduce the dimensions (e.g., 512 layers to 10 modes observed at 22:00UTC at 90% variance truncation) for radar reflectivity profiles and extracts at most 10 uncorrelated, independent random variables. Thus, the normally distributed perturbation is added on the modes of sample-mean of radar reflectivity profiles based on the equation (2). We utilize Problem Solving environment for Uncertainty Analysis and Design Exploration toolkit (PSUADE)[*Tong*, 2009] to provide spatial and temporal UQ results for MICROBASE. Comparison of mean values and standard deviation of our UQ results (5000 runs) with the ensemble average of original MICROBASE simulation results is displayed in Figure 1 (b) – (d). It shows that mean values of our UQ results is similar to the direct ensemble average with the same degree of magnitude. The standard deviations of IWC in our UQ results is around 1/5 of the corresponding mean values during the IOP on 9 March 2000.

Using our UQ methodology, the average (min, max) values of the IWP retrieved by MICROBASE (unit: $\mathrm{g/m^2}$) are 21.9 (2.4, 54.5). These numbers fall into the range of results from 14 different retrievals shown in Table 2 in [*Comstock et al.*, 2007] (average numbers are 16.4 (0.076, 63.3)), indicating that the uncertainties quantified in both studies are consistent. It highlights the fact that propagating the uncertainties in the input data as well as the parameters through a single retrieval (i.e., MICROBASE) leads to the uncertainties in the output comparable to the differences amongst different retrievals as discussed in [*Comstock et al.*, 2007], many of which are rooted from different theories/hypotheses and even based on different instruments. This implies that it might be possible to partly reconcile different algorithms by understanding the causes of the uncertainty in one of them. For instance, the uncertainty in the IWP retrieved by MICROBASE is mainly attributed to radar reflectivity profiles in this one-day case (see the Sobol' sensitivity analysis below). Thus, the retrieval differences may be largely caused by how differently radar reflectivity profiles is utilized by different algorithms.

Comparisons with independent observations (e.g., aircraft) provide another way to interpret our method. Figure 1 (e) compares the IWP from the counterflow virtual impactor (CVI) ([*Twohy et al.*, 1997], black line) observation on the aircraft, original MICROBASE (red line), and our results (blue line). In general, the average of in situ CVI measurements are greater than both retrievals and they agree within a factor of two. The differences between observations and retrievals are partly due to different sampling volumes, instrument uncertainties, sensitivities, and limitations ([*Comstock et al.*, 2007]). In addition, we note that our average values are closer to the CVI probe than the original MICROBASE, which suggests the possibility of using our method to improve the retrievals. This improvement is probably mainly because our methodology parameterizes the input measurements based on the facts that (1) KLE constructs uncorrelated orthogonal bases and the autocorrelation kernel is relatively stable; and (2) sample mean is a more smooth statistical variable and follows normal distribution per CLT. In other words, we replace the model input of finite observations with infinite random fields. Therefore, our expectations of model output are likely closer to the reality than the original algorithm.

The vertical bars in Figure 1 (e) are defined differently. The CVI bars (black) represent the standard deviations (STDs) of the mean IWP of the 2-min observations when the aircraft flew over the SGP site. The raw MICROBASE bars (red) depict the standard error of the mean (SEM) in 0.5 hour, while those of our results (blue) represent the STD of sample mean in 0.5 hour. It would be better to plot the same quantity for comparison. We opt to use different quantities because we do not have access to the number of CVI observations to calculate its SEM. The bars of CVI and raw MICROBASE generally overlap, which is consistent with results found in [*Comstock et al.*, 2007]. The uncertainties quantified by our method are much smaller because (1) it estimates the uncertainty for the sample mean which smooths out the uncertainties; (2) the IWC retrieval formula above is quite simple and hence we cannot perturb all the uncertainty sources; and (3) the bars of CVI and raw MICROBASE denote the variability of limited realizations rather than the uncertainty.

Figure 2 (a) displays the PDF of IWC at 8km within different time windows. The retrievals exhibit larger spread in the probability distribution of ice water path (IWP) for the optically thin clouds as shown in Figure 2 (b) and (c). In particular, mean value and standard deviation of IWP at 21:00UTC is around 50.8 and 1.1, respectively, while mean value and standard deviation of IWP at 22:00UTC is 2.8 and 0.13, respectively. So the coefficient of variance defined as fraction of standard deviation over mean is 0.02 and 0.05 for IWP at 21:00UTC and 22:00UTC, respectively. Therefore, IWP retrieved by MICROBASE incurred more than twice of coefficient of variance in optically thin ice clouds (22:00UTC) compared with the one in optically thick ice clouds (21:00UTC) due to uncertainty in observations and key parameters. On the other hand, IWC retrieved by MICROBASE at 8km has larger standard deviation at 21:00UTC than the one obtained in 22:00UTC, which suggests large variability in vertical in the retrieved IWC.

4. Discussions and Conclusions

Many previous studies aim to understand and quantify the uncertainties in cloud retrievals (e.g., [*Comstock et al.*, 2007; *Turner et al.*, 2007; *Zhao et al.*, 2014]). The primary purpose of this study is to establish a novel observation-based methodology to generally quantify the retrieval uncertainties for model evaluation (especially global models). Despite that many existing methods can only estimate column-integrated uncertainties, our unique method also performs vertically resolved UQ analysis. The vertical UQ structure is often more desirable for model evaluation as vertical structures of clouds are essential to many topics such as radiative forcing and climate change. To reduce the dimensionality of random inputs, our method takes into account the correlation between vertical layers in the input data by adopting the KL expansion. Moreover, by eliminating the assumption that different layers are uncorrelated, the output uncertainty range becomes more accurate and reliable. Besides means and standard deviations, this method also quantifies the full probabilistic distribution functions (PDFs) of retrieved quantities. This observation-based PDFs information can be used as the *a-priori* for the Bayesian approach (e.g., [*McFarlane et al.*, 2002; *Posselt et al.*, 2008]) so as to avoid the subjective error introduced by assuming a priori PDF (usually uniform), and hence the results from such Bayesian studies will be improved and more meaningful.

Besides propagating uncertainties in the input data and the parameters, this UQ approach has the capability of attributing the output uncertainties to individual error source. This capacity is particularly useful when dealing with highly non-linear retrieval algorithms, as different error sources are more likely entangled. Figure 3 (a)–(d) show the results of Sobol' first and group sensitivity analysis for IWC at 8 km (left column) and IWP (right column) on March 9, 2000. No main-effect is found from the perturbation of each single mode of radar reflectivity profiles and the parameter a (see Figure 3 (a) and (c)). However, the contributions from the entire group of radar reflectivity profiles modes are added up to almost one (see Figure 3 (b) and (d)). These results suggest that the uncertainties in the IWC and IWP are mainly due to the interactions of different modes of radar reflectivity profiles. The Sobol' second sensitivity analysis of IWP at 21:00-21:30 UTC and 22:00-22:30 UTC (see 3 (d) and (f)) confirms this finding. In particular, the mode interaction of radar reflectivity profiles is stronger for the optically thin clouds observed at 22:00-22:30 UTC than other periods such as at 21:00-21:30 UTC. Such quantitative knowledge about the relative contribution of individual error source to the output uncertainties provides valuable insights and clues to improve the retrieval algorithm and measurements.

Despite of the above advantages, this framework does not cover all the aspects of UQ analysis. For example, it cannot quantify systematic biases and the structure uncertainty (i.e., the model formula). The parameters of the retrieval algorithm may not be independent as assumed in this approach, for instance, a and b in the formula $IWC = aZe^b$ [*Matrosov*, 1999]. In addition, some retrievals (e.g., [*McFarlane et al.*, 2002; *Turner*, 2005; *Posselt et al.*, 2008]) already apply the uncertainty estimation theory, and thus our approach may not be able to be directly applied to such algorithms.

5. Future Outlook

The case study in this paper mainly demonstrates the capacities of this newly developed UQ methodology. We will expand the UQ analysis to long-term ARM observations to include different seasons, locations, cloud types, etc. Such comprehensive knowledge about retrieval uncertainties will facilitate the application of retrieval products in model evaluation and can be used to improve instruments, observation strategies as well as retrieval algorithms. We also plan to exploit the uncertainties of other retrieval algorithms. Using multi-retrieval and global model observations, we can further apply multi-model calibration technique to mitigate the uncertainty estimated by each retrieval algorithm.

Acknowledgments. This work is mainly supported by the DOE Atmospheric Radiation Measurement program, the Atmospheric System Research Quantification of Uncertainty in Cloud Retrieval session, and partially supported by the Chinese program for New Century Excellent Talents in University (NCET) and the Fundamental Research Funds for the Central Universities. This work was performed under the auspices of the U.S. Department of Energy by Lawrence Livermore National Laboratory under Contract No. DE-AC52-07NA27344. The authors would like to thank the help from Michael Jensen, Matthew Macduff, Laura Riihimaki, Chitra Sivaraman, Timothy Shippert, and Charles Tong.

Appendix A

Subtracting ensemble mean $\bar{y}(\mathbf{x})$ from each snapshot, we obtain a zero-mean $N \times n$ snapshot matrix

$$\mathbf{Y} = [y_1 - \bar{y}, y_2 - \bar{y}, \ldots, y_n - \bar{y}] \tag{A1}$$

It should be noted that we take snapshots of relative error for radar reflectivity profiles and LWP, i.e., the snapshot matrix above is divided by $\bar{y}$, for which corresponding formulas can be derived similarly.

Without loss of generalization, the following

$$\Psi = \{\psi_1, \psi_2, \ldots, \psi_M\} \tag{A2}$$

of order $M \leq n$ provides an optimal representation of the ensemble data in a $M-$dimensional subspace by minimizing the averaged projection error

$$\min_{\{\psi_1,\psi_2,\ldots,\psi_M\}} \frac{1}{n}\sum_{i=1}^{n} \left\|(y_i - \bar{y}) - \Pi_{\Psi,M}(y_i - \bar{y})\right\|^2$$
$$\text{s.t. } \langle \psi_i, \psi_j \rangle = \delta_{ij} = \begin{cases} 1 & i = j \\ 0 & i \neq j \end{cases} \tag{A3}$$

where $\langle \cdot, \cdot \rangle$ represents an inner product, $\Pi_{\Psi,M} = \sum_{i=1}^{M} \langle y_i - \bar{y}, \psi_i \rangle \psi_i$ is the projection operator onto the M-dimensional space spanned by Ψ.

To compute the KLE modes $\psi_i \in \mathbb{R}^N$ satisfying Eq. (A3), one solves an $N-$dimensional eigenvalue problem

$$\mathbf{A}\psi_i = \lambda_i \psi_i \tag{A4}$$

where $\mathbf{A} = \mathbf{Y}\mathbf{Y}^{\mathbf{T}}$ is the spatial correlation matrix.

Since in practice the number of snapshots is much less than the the state dimension, $n << N$, an efficient way to compute the reduced basis is to introduce a $n-$dimensional matrix $\mathbf{K} = \mathbf{Y}^{\mathbf{T}}\mathbf{Y}$ and compute the eigenvalues $\lambda_1 \geq \lambda_2 \geq \ldots \geq \lambda_n \geq 0$ of $\mathbf{K}$ with its corresponding eigenvectors $\phi_1, \ldots, \phi_n$. The corresponding KLE modes are thus obtained by

$$\psi_i = \frac{1}{\sqrt{\lambda_i}} \mathbf{Y} \phi_i, \quad i = 1, \ldots, M \tag{A5}$$

where $\langle \psi_i, \psi_j \rangle = \delta_{ij}$.

One can define a relative information content to choose a low-dimensional basis of size $M << n$ by neglecting modes corresponding to the small eigenvalues. We define

$$I(m) = \frac{\sum_{i=1}^{i=m} \lambda_i}{\sum_{i=1}^{i=n} \lambda_i} \tag{A6}$$

and choose M such that $M = \arg\min \{I(m) : I(m) > \gamma\}$, where $0 \leq \gamma \leq 1$ is the percentage of total information retained in the reduced space and the tolerance γ must be chosen to be close unity in order to capture most of the energy of the snapshots basis.

To sum up, we obtain that each one observation y_i can be expanded in terms of M numbers of KLE modes written as

$$y_i = \bar{y} + \sum_{i=1}^{M} \psi_i \sqrt{\frac{\lambda_i}{n}} V_i \tag{A7}$$

where modal coefficients V_i computed by $V_i = \psi_i^{\mathbf{T}} y_i \sqrt{\frac{n}{\lambda_i}}$ and $\langle V_i, V_j \rangle = \delta_{ij}$.

Since mean is subtracted from each snapshots, it can be shown that $\frac{1}{n}\sum_{j=1}^{n} (V_{ij}) = 0$, where V_{ij} corresponds to the observation $y_j - \bar{y}$ projected onto the mode ψ_i.

As a result, $Y(\mathbf{x}, t, \theta)$ can be approximated by KLE to the order of M as

$$Y(\mathbf{x}, t, \theta) = \bar{y} + \sum_{i=1}^{M} \psi_i \sqrt{\frac{\lambda_i}{n}} \xi_i \tag{A8}$$

such that $E(\xi_i) = 0$ and $E(\xi_i \xi_j) = \delta_{ij}$, $i = 1, \ldots, M$, and ξ_i follows some unknown distribution.

Appendix B

Let $w = [w_1, w_2, \ldots, w_N]^{\mathbf{T}}$ be a time independent spatial Gaussian noises injected into each one observation y_i, such that w follows a multivariate normal distribution defined as $w \sim \mathcal{N}\left(0, \sigma_0^2 \mathbf{I}_N\right)$ and $\mathbf{I}_N$ is a $N \times N$ identity matrix. Since Ψ is orthogonal transformation, Ψw follows the same distribution as w, i.e., $\Psi w \sim \mathcal{N}\left(0, \sigma_0^2 \mathbf{I}_N\right)$. Therefore, without loss of generalization, adding Ψw to the Equation (A8) and truncating it to the order of M, we obtain that

$$\begin{aligned} Y'(\mathbf{x}, t, \theta) &= Y(\mathbf{x}, t, \theta) + \Psi w \\ &= \bar{y} + \sum_{i=1}^{M} \psi_i \sqrt{\frac{\lambda_i}{n}} \xi_i + \sum_{i=1}^{M} \psi_i w_i \\ &= \bar{y} + \sum_{i=1}^{M} \psi_i \sqrt{\frac{\lambda_i}{n}} \left(\xi_i + \frac{w_i}{\sqrt{\frac{\lambda_i}{n}}} \right), \end{aligned} \tag{B1}$$

where $Y'(\mathbf{x}, t, \theta)$ is a stochastic process representing noisy observations, w_i is the i-th component of the truncated random vector Ψw.

Let ζ_i be $\zeta_i = \xi_i + \frac{w_i}{\sqrt{\frac{\lambda_i}{n}}}$, we obtain

$$Y'(\mathbf{x}, t, \theta) = \bar{y} + \sum_{i=1}^{M} \psi_i \sqrt{\frac{\lambda_i}{n}} \zeta_i \tag{B2}$$

where $E(\zeta_i) = 0$ and $Var(\zeta_i) = \sqrt{1 + \left(\frac{\sigma_0}{\sqrt{\frac{\lambda_i}{n}}} \right)^2}$.

Taking average on both sides, it can be rewritten as

$$\overline{Y'}(\mathbf{x}, t, \theta) = \bar{y} + \sum_{i=1}^{M} \psi_i \sqrt{\frac{\lambda_i}{n}} \overline{\zeta_i} \tag{B3}$$

Finally, based on CLT, we have

$$\overline{Y'}(\mathbf{x},t,\theta) = \bar{y} + \sum_{i=1}^{M} \psi_i \sqrt{\frac{\lambda_i}{n}} \sqrt{1 + \left(\frac{\sigma_0}{\sqrt{\frac{\lambda_i}{n}}}\right)^2} \frac{z_i}{\sqrt{n}} \tag{B4}$$

where $z_i \sim \mathcal{N}(0,1)$.

References

Comstock, N. M., R. D. Entremont, D. Deslover, and C. G. Mace (2007), An intercomparison of microphysical retrieval algorithms for upper tropospheric ice clouds, *Bull. Am. Meteorol. Soc*, *88*, 191–204.

Dunn, M., K. L. Johnson, and M. P. Jensen (2011), The microbase value-added product: A baseline retrieval of cloud microphysical properties, *Tech. rep.*, DOE ARM.

Hotelling, H. (1933), Analysis of a complex of statistical variables into principal components, *Journal of Educational Psychology*, *24*(1), 417–441,498–520.

Kosambi, D. D. (1943), Statistics in function space, *J. Indian Math. Soc.*, *7*(1), 559–572.

Kuhunen, K. (1947), Uber lineare methoden in der wahrscheinlichkeitsrechnung, *Am. Acad. Sci.*, *37*, 3–79.

Loéve, M. (1945), Fonctions aleatoires de second ordre, *C. R. Acad. Sci.*

Matrosov, S. Y. (1999), Retrievals of vertical profiles of ice cloud microphysics from radar and IR measurements using tuned regressions between reflectivity and cloud parameters, *J. Geophys. Res.*, *104*(D14), 16,741–16,753, doi:10.1029/1999JD900244.

McFarlane, S. A., K. F. Evans, and A. S. Ackerman (2002), A bayesian algorithm for the retrieval of liquid water cloud properties from microwave radiometer and millimeter radar data, *J. Geophys. Res.*, *107*(D16), 4317, doi:10.1029/2001JD001011.

McKay, M. C., R. Beckman, and W. Conover (1979), A comparison of three methods for selecting values of input variables in the analysis of output from a computer code, *Technometrics*, *21*(2), 239–245.

Pearson, K. (1901), On lines and planes of closest fit to systems of points in space, *Philosophical Magazine*, *2*(1), 559–572.

Posselt, D. J., T. S. L'Ecuyer, and G. L. Stephens (2008), Exploring the error characteristics of thin ice cloud property retrievals using a Markov chain Monte Carlo algorithm, *J. Geophys. Res.*, *113*(D24), D24,206, doi:10.1029/2008JD010832.

Ross, S. (2010), *A first course in probability*, Pearson.

Sirovich, L., J. L. Lumley, and G. Berkooz (1987), Turbulence and the dynamics of coherent structures, part iii: dynamics and scaling, *Quarterly of Applied Mathematics*, *45*(3), 583–590.

Sobol, I. (1993), Sensitivity estimates for nonlinear mathematical models, *MMCE*, *1*(4), 407–414.

Tong, C. (2009), *PSUADE User's Manual (Version 1.2.0)*, Lawrence Livermore National Laboratory, lLNL-SM-407882.

Turner, D. D. (2005), Arctic mixed-phase cloud properties from AERI lidar observations: Algorithm and results from SHEBA, *J. Appl. Meteor.*, *44*(4), 427–444, doi:10.1175/JAM2208.1.

Turner, D. D., S. A. Clough, J. C. Liljegren, E. E. Clothiaux, K. Cady-Pereira, and K. L. Gaustad (2007), Retrieving liquid water path and precipitable water vapor from atmospheric radiation measurement (arm) microwave radiometers, *IEEE Trans. Geosci. Remote Sens.*, *45*(11), 3680–3690.

Twohy, C. H., A. J. Schanot, and W. A. Cooper (1997), Measurement of condensed water content in liquid and ice clouds using an airborne counterflow virtual impactor, *J. Atmos. Oceanic Technol.*, *14*(197-202).

Xie, S. (2011), Focus group proposal whitepaper: Asr quantification of uncertainty in cloud retrievals (quicr) focus group, *Tech. rep.*, DOE coud retrievals focus group.

Zhao, C., S. Xie, and K. A. Stephen (2012), Toward understanding of differences in current cloud retrievals of arm ground-based measurements, *J. Geophys. Res. Atmos.*, *117*(D10), 1–21.

Zhao, C., S. Xie, X. Chen, M. P. Jensen, and M. Dunn (2014), Quantifying uncertainties of cloud microphysical property retrievals with a perturbation method, *J. Geophys. Res. Atmos.*, *119*, 1–11.

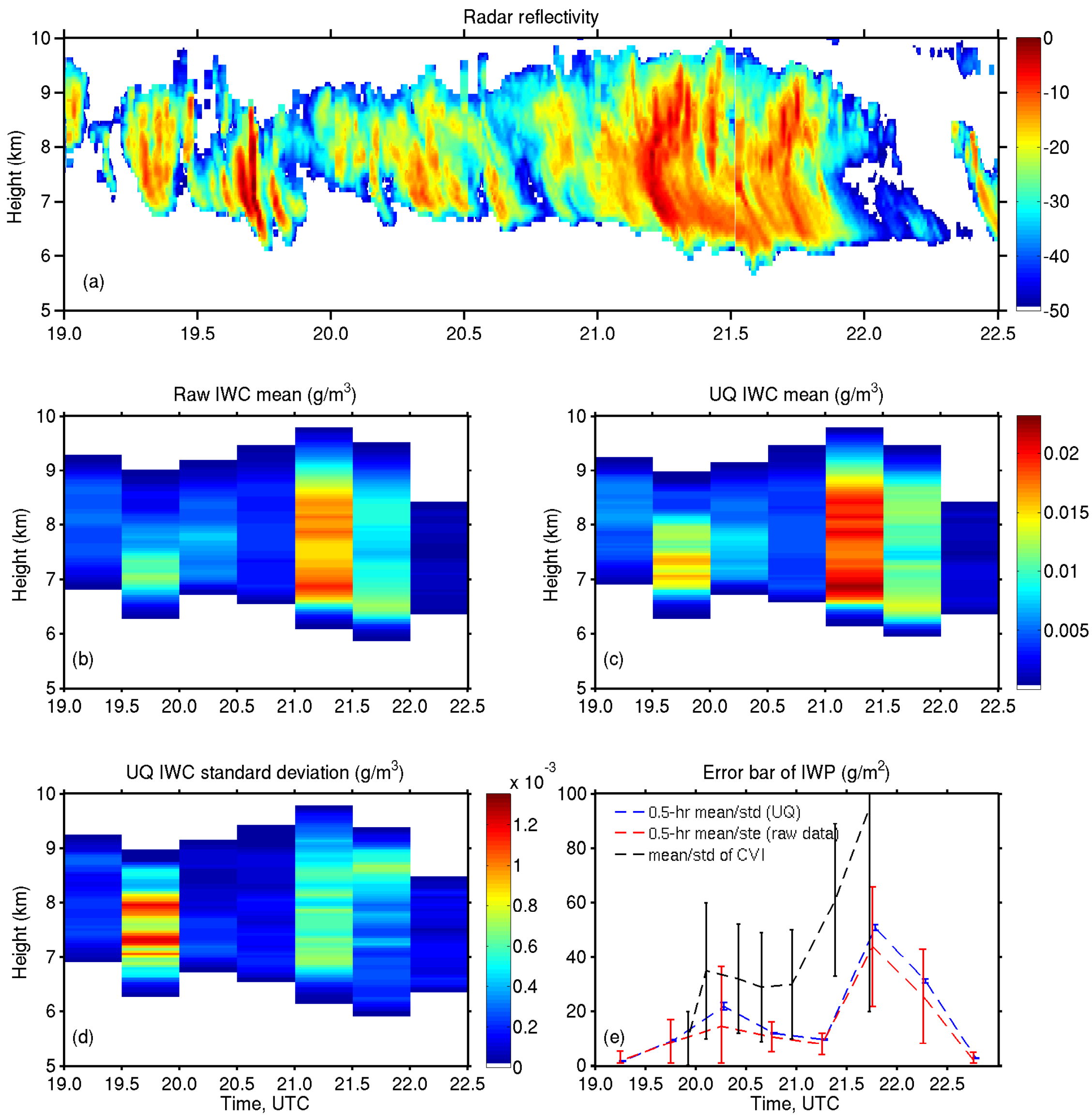

Figure 1. (a) MMCR reflectivity (dBZ); (b) Ensemble average of raw MICROBASE retrieved IWC; (c) Mean values, and (d) standard deviations of applying our UQ method to IWC, respectively; (e) Comparison of 0.5-hour mean/standard deviations of IWP by applying our UQ method, 0.5-hour mean/standard error of raw MICROBASE retrieved IWP, and in-situ (CVI) 2-min mean/standard deviations of IWP as aircraft passed over the SGP CRF.

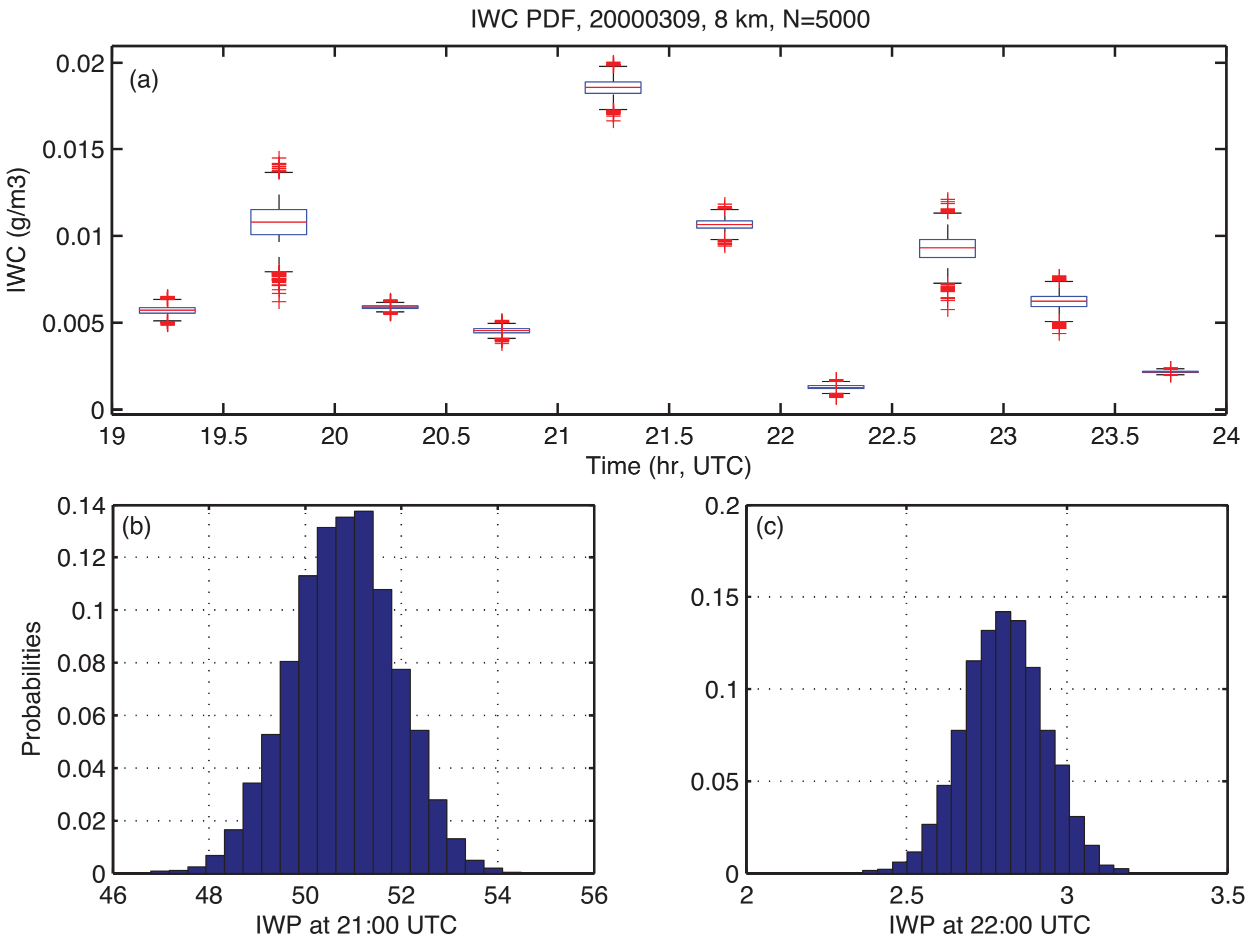

Figure 2. (a) Box-plot of IWC at 8km, and probability density function plot of IWP observed at (b) 21:00UTC and (c) 22:00UTC on 9 Mar 2000, respectively.

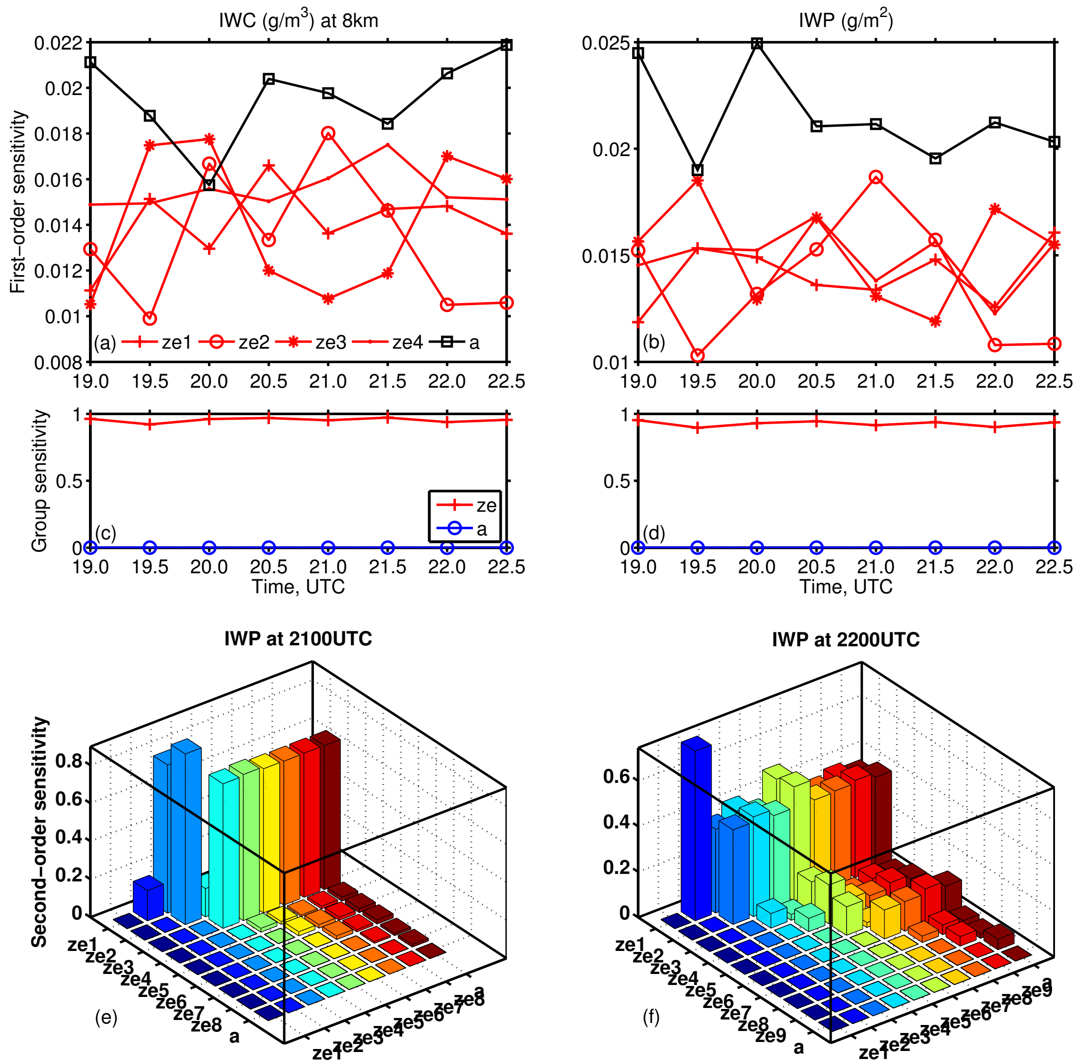

Figure 3. Sobol' first-order sensitivity analysis of (a) IWC at 8km and (b) IWP, respectively; Sobol' group sensitivity analysis of (c) IWC at 8km and (d) IWP, respectively; Sobol' second-order sensitivity analysis of IWP at (e) 21:00UTC and (f) 22:00UTC, respectively; Figures (a) - (f) are plotted between 21:00UTC and 22:00UTC on 9 Mar 2000.